CHEMISTRY
A EUROPEAN JOURNAL

DOI: 10.1002/chem.200700860

Effective Enhancement of Fluorescence Signals in Rotaxane-Doped Reversible Hydrosol–Gel Systems

Liangliang Zhu, Xiang Ma, Fengyuan Ji, Qiaochun Wang, and He Tian*[a]

Dedicated to Professor Daoben Zhu on the occasion of his 65th birthday

Abstract: Rotaxane-based nanoscale architectures have a huge potential to be processed into widely applied devices. In this work, light-driven rotaxanes with fluorescent chromophores based on α-cyclodextrin (α-CyD) have been doped into amphoteric thermoreversible hydrosol–gels to form a new type of disperse system with reversible optical signals. The photoisomerizations with α-CyD shuttling have been studied by induced circular dichroism (ICD). Compared with their corresponding solutions, the rotaxane-doped hydrosol–gel systems produce much more obvious fluorescent binary signals.

Keywords: cyclodextrins · fluorescence · hydrosol–gel · photoisomerization · reversible systems · rotaxanes

Introduction

"Moving and working like machines" is a goal that many nanoscientists have been embracing and pursuing for years. Some supramolecular machines and devices[1] are showing an increasingly greater potential for applications in areas such as molecular switches,[2] molecular logic gates,[3] molecular wires,[4] and information storage.[5] Rotaxane,[6] one of the typical interlocked supramolecular systems, has been developed extremely fast in recent years due to its challenging constructions and unique functions. Recently, several α-CyD-based rotaxanes containing one or two fluorescent naphthalimide units as stoppers have been synthesized by our group.[7] These rotaxanes could be regarded as good models for binary systems because of their variable and reversible output signals originating from different inputs. Thus far, most researchers including ourselves believe that lots of charming performances of switchable rotaxanes can be easily revealed in solution. However, incoherence and physical instability of the solution state hinders these types of materials from being extensively applied.

To overcome these obstacles, many efforts have been made, such as transforming supramolecular systems into solid states,[8] Langmuir–Blodgett films,[9] and self-assembly monolayers.[10] Good results have been attained by these methods to some extent, but the disadvantages of a low conversion rate or of the inconvenience of the transformation also exist. Compared with these morphologies mentioned above, the low-molecular-weight gelator (LMWG)[11]-formed thermoreversible sol–gel system has its own merits. As a kind of mesophase, a sol–gel system has high flexibility and workability. Furthermore, these easily prepared systems are generally more retentive than solutions so as to be favorable to storage and transportation.

We have focused on seeking other suitable media for supramolecules to improve their performances and to investigate their special characteristics. Herein, a fitting amphoteric thermoreversible hydrosol–gel system[12] without visible absorption or strong scattering was chosen. Two samples R1 and R2 were dispersed at 60 °C to form rotaxane-doped hydrosol systems R1-Sol and R2-Sol, respectively (Figure 1). Their references (R1-Ref-Sol and R2-Ref-Sol) were prepared in the same way. These hydrosol systems could be changed into their corresponding hydrogels by cooling to room temperature and heating back into hydrosols reversibly (Figure 2). The induced circular dichroism (ICD) performances of these rotaxanes in aqueous solution and hydrosol systems were investigated for their conformational

[a] L. Zhu, X. Ma, F. Ji, Q. Wang, Prof. H. Tian
Key Laboratory for Advanced Materials and
Institute of Fine Chemicals
East China University of Science and Technology
Shanghai 200237 (P.R. China)
Fax: (+86) 21-6425-2288
E-mail: tianhe@ecust.edu.cn

Supporting information for this article is available on the WWW under http://www.chemeurj.org/ or from the author.

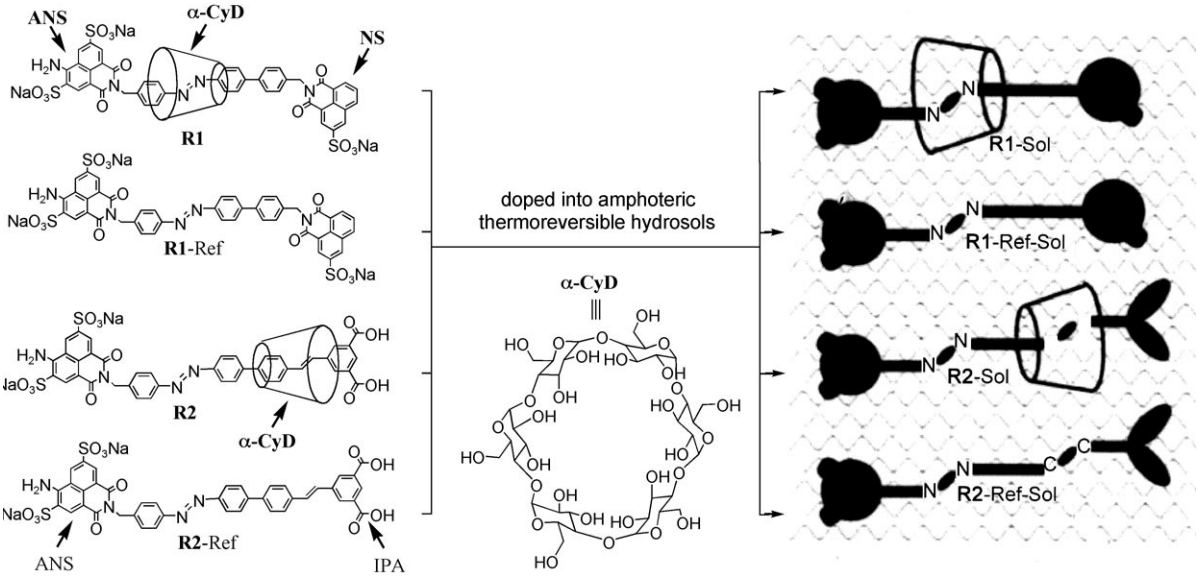

Figure 1. The structures of light-driven rotaxanes **R1** and **R2** and their references. ANS = 4-Amino-1,8-naphthalimide-3,6-disulfonic disodium salt, NS = 1,8-naphthalimide-3-sulfonic sodium salt, IPA = isophthalic acid.

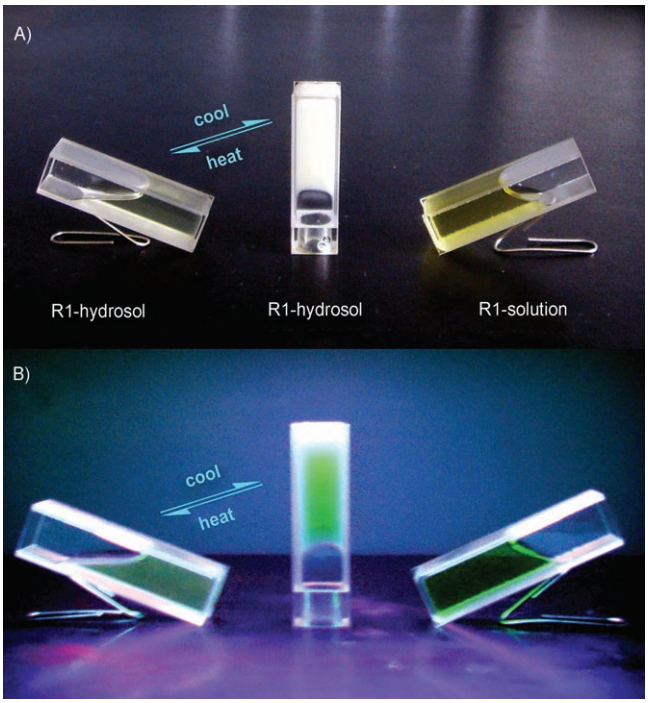

Figure 2. Images of **R1**-doped hydrosol, hydrogel, and aqueous solution (A) and the samples under irradiation at 365 nm (B).

identifications. Clearly improved optical performances were observed by fluorescence spectroscopy. It is obvious that a novel fluorescence-enhanced thermoreversible system is achieved in this work and its output fluorescent signals are also reversible as the corresponding solution.

Results and Discussion

Shuttling motion with photoisomerization: The fact that a α-CyD macrocycle can shuttle along the dumbbells due to the photoisomerization of azobenzene or stilbene units has been confirmed by ^{1}H NMR and 2D ROESY NMR spectrsocopy in these structures.[2a,3d] ICD spectra, another effective method to detect chirality or optical activity, can describe the co-conformations with shuttling movements of α-CyD in detail.[13] ICD signals of an achiral guest chromophore originate when it is located in a chiral environment like a CyD host. According to the general rule,[14] a positive/negative ICD signal arises when the electric transition dipole moment of the guest inside the host cavity is aligned parallel/perpendicular to the axis of the chiral host. On the contrary, the sign of the ICD signal is just opposite when the electric transition moment of the guest is outside the host cavity. The ICD signal converges to zero when the angle between the transition moment and the CyD axis turns to 54.7°. Thereby, the variations of ICD signals directly reflect their angles and positions.

The ICD spectra with respect to the photoisomerization of the **R1**-aq solution and the **R1**-doped hydrosol are shown in Figure 3. It has been confirmed that the irradiation of the aqueous **R1** solution at 365 nm induces *E* to *Z* photoisomerization, and the α-CyD ring moves from the azo unit to the biphenyl unit. In the initial state, the azo unit located in the cavity of α-CyD and its $\pi < \mathrm{Pl} > \pi^*$ transition has an absorption maximum at 360 nm while the one at 430 nm is mainly attributed to the superposition of the $n < \mathrm{Pl} > \pi^*$ transition of the azo unit and ANS unit. These units are involved in the chiral environment of the α-CyD cavity so as to give ICD signals at wavelengths corresponding to their visible absorptions.

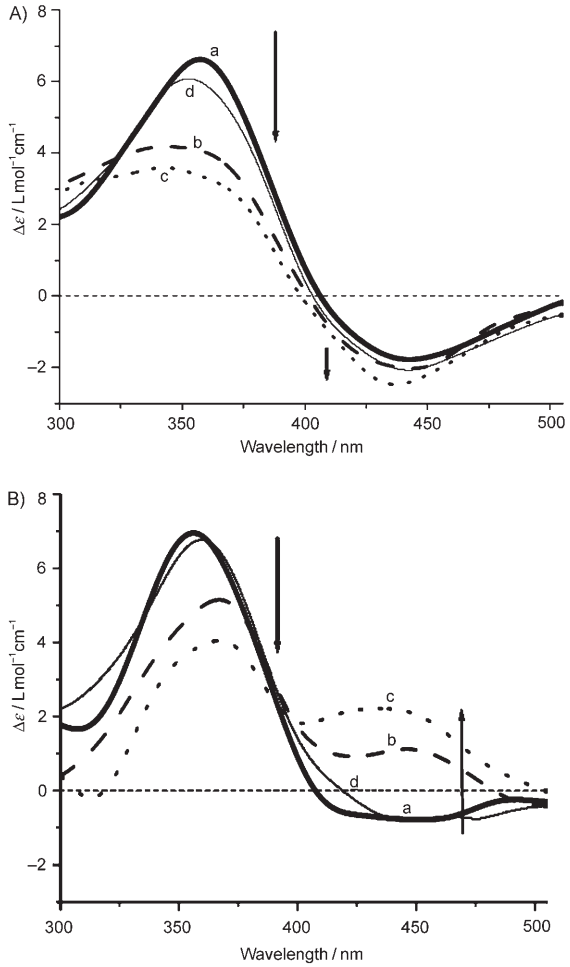

Figure 3. A) ICD spectral changes for **R1**-aq solution (25 °C, 1.0×10^{-4} M; a) 0 min, b) 3 min, c) 15 min, d) 30 min-back) and B) **R1**-doped hydrosol with a 10% gelator content (40 °C, 1.0×10^{-4} M; a) 0 min, b) 5 min, c) 20 min, d) 40 min-back) by irradiation at 365 nm. The spectral change can be reversed back to its original state by irradiation at 254 nm.

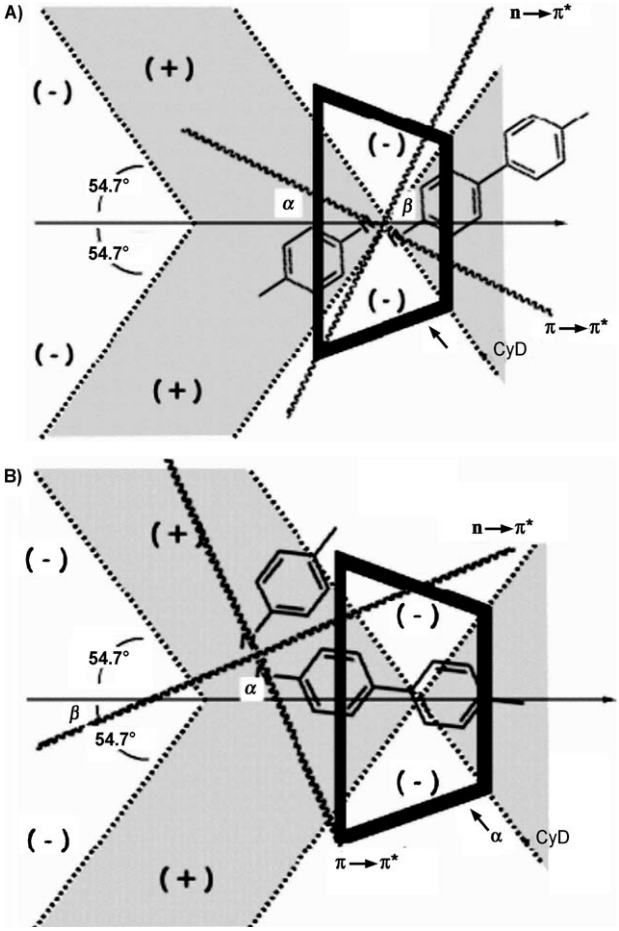

Figure 4. Relationship of the angles α and β and positions between the α-CyD ring and the linear subunit before (A) and after (B) the photoisomerization of the azo unit in **R1**-aq solution. α is the angle between the axis and the orientation of the π<Pl>π * transition while β is the angle between the axis and the orientation of the n<Pl>π* transition.

The absorption of **R1**-sol occurs at more or less the same position as **R1**-solution due to the physical adsorption between the dopant molecules and micelles. The ANS and NS units are far away from the chiral cavity of α-CyD so that the ICD spectral changes are mainly induced by the variations of angles α or β, marked between the axis and the orientation of π<Pl>π* or the n<Pl>π* transition, respectively. A possible case we inferred is shown in Figure 4. For **R1**-aq solution, a strong positive Cotton effect arises when a π<Pl>π* transition is located in the cavity of α-CyD with an α value far smaller than 54.7°. The π<Pl>π* transition occurs outside of the cavity after the photoisomerization and α becomes slightly bigger than 54.7°. Thus, the $\Delta\varepsilon$ value at 360 nm, a reflection of statistical regularity, decreases from 6.6 to 3.3 $L\,mol^{-1}\,cm^{-1}$. Meanwhile, the n<Pl>π* transition lies in both the regions in which a negative Cotton effect appears before and after the photoisomerization. However, β becomes farther away from 54.7°, namely, the absolute value of β minus 54.7° gets bigger. Thus a more negative ICD signal is given and the $\Delta\varepsilon$ at 430 nm declines from −1.5 to −2.3 $L\,mol^{-1}\,cm^{-1}$.

An obvious difference appears at the peak of 430 nm of **R1**-sol compared with **R1**-solution. The adsorption in hydrosol makes it more difficult for the photoisomerization of the azo unit of **R1** as well as the shift of α-CyD. After irradiation for 20 min, α-CyD might not depart from azobenzene completely and the n<Pl>π* transition seems to still take place in the cavity. However, the orientation of n<Pl>π* becomes parallel to the axis (β was less than 54.7°) so that a positive Cotton effect is produced (see Figure 5). Irradiation at 254 nm causes the *Z* form to return to the *E* form both for **R1**-sol and **R1**-solution with the recovery of their ICD signals.

The ICD spectra of **R2**-alkaline (10 mol equivalents of sodium carbonate added) aq solution and -hydrosol are described in Figure 6. In these two systems, azobenzene and stilbene are both in the *E* form with α-CyD mostly located in the stilbene unit (*EE* state). *E*-to-*Z* photoisomerization of the azobenzene (*ZE* state) will happen by irradiation at 380 nm alone, while the irradiation at 313 nm causes *E*-to-*Z*

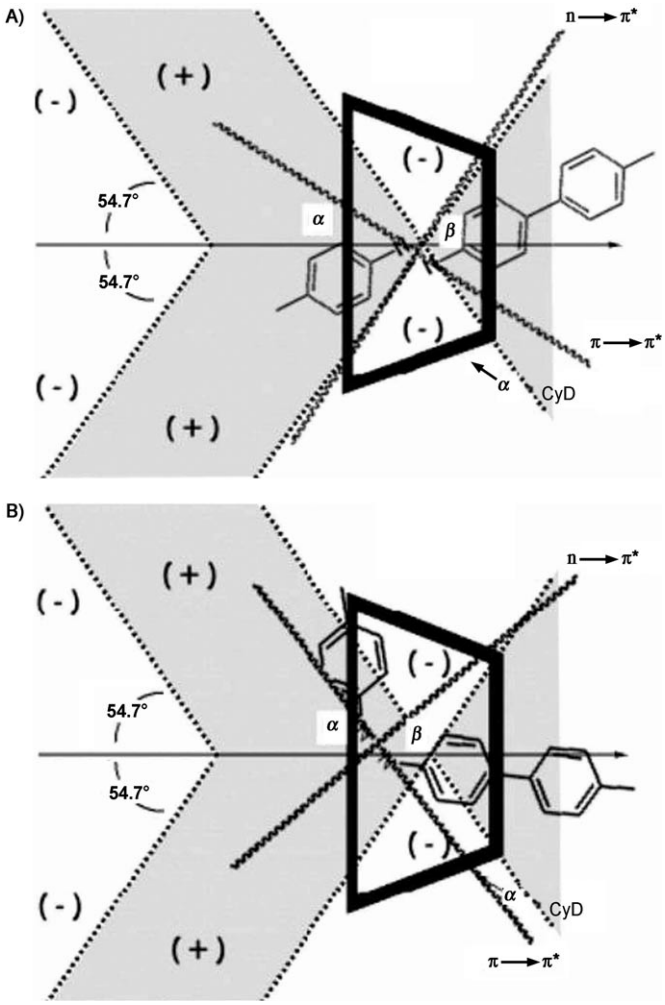

Figure 5. Relationship of the angles α and β and positions between the α-CyD ring and the linear subunit before (A) and after (B) the photoisomerization of the azo unit in **R1**-doped hydrosol.

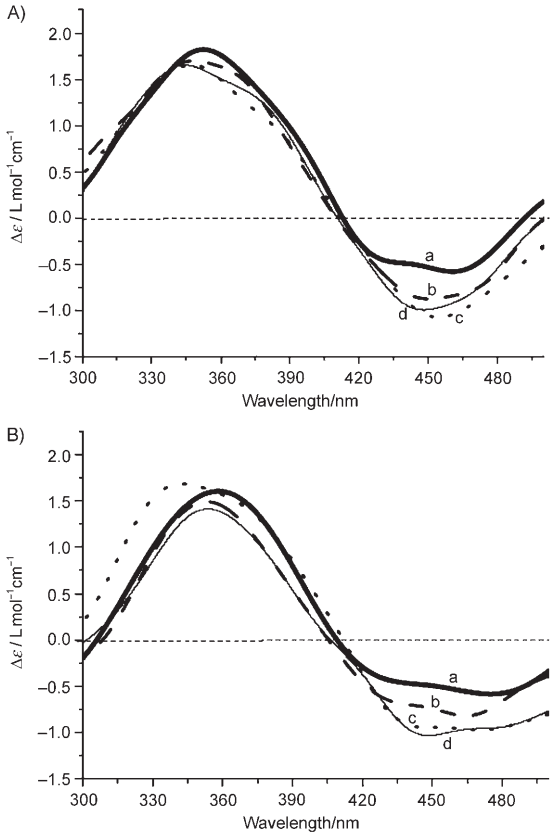

Figure 6. ICD spectra of four states of **R2**-alkaline aq solution (1.0×10^{-4} M, 25 °C) (A) and **R2**-alkaline hydrosol with a 10 % gelator content (1.0×10^{-4} M, 40 °C) (B). a) *EE*, b) *ZE*, c) *EZ*, d) *ZZ*.

photoisomerization of stilbene (*EZ* state). The two units will both be isomerized (*ZZ* state) with irradiation at 313 and 380 nm, successively.[3d] Corresponding movements of α-CyD will take place with the photoisomerizations of these units. Isomerized stilbene and azobenzene can recover to the *E* form by irradiation at 280 and 450 nm, respectively. The Cotton effects of isoconcentrated **R2** generate in similar positions to that of **R1** with weaker signals at 360 nm ($\Delta\varepsilon <$ 2 L mol^{-1} cm^{-1}). The positive Cotton effect of *ZE*, *EZ*, and *EE* states blue shifts to less than 350 nm as a result of the fact that the conjugated π system becomes weaker when any photoisomerizable unit turns to the *Z* form. Nevertheless, the intensity of the ICD signal changes little because the α-CyD ring shuttles along the whole π system containing stilbene but never locates on the azo unit completely. The shortened distance between the ANS unit and α-CyD with *E*-to-*Z* photoisomerization of stilbene produced a slightly stronger negative ICD signal at 450 nm ($\Delta\varepsilon$ of *EZ* state is −1.05 L mol^{-1} cm^{-1}). The ICD spectral change of **R2**-sol is similar to that of **R2**-solution integrally.

Effective enhancement of fluorescence signals in hydrosol–gel systems: Fluidity of water is confined by a synergistic effect of hydrophilic and hydrophobic groups in amphoteric micelles. Hence, the performances of dopants dissolved in the water phase can also be influenced by gelators. The gelator we chose can form a hydrosol–gel with water in a large range of concentrations. We dispersed the same amount of **R1** into hydrosols of different gelator contents (wt %) to determine the fluorescent enhancement effect.

The fluorescent intensities at 520 nm of **R1**-doped hydrosol systems (Figure 7b–e) are obviously higher than that of **R1**-aq solution (Figure 7a). After removing the Tyndall scattering of the hydrosol itself (Figure 7f), we could find that the net fluorescent intensities of the dopant are still stronger than that of solution. The net fluorescent intensity grows with the increase of the gelator content (for example, the net fluorescent intensity of **R1**-doped hydrosol with 20 % gelator content has reached three times more than that of **R1**-aq solution). The enhancement of fluorescent intensity should be attributed to the adsorption of parts of sample molecules on the micellar surfaces. In this way, fluorescent quenching, induced by the collisions between sample molecules or the collisions between a sample molecule and the amphoteric micelles, is reduced.

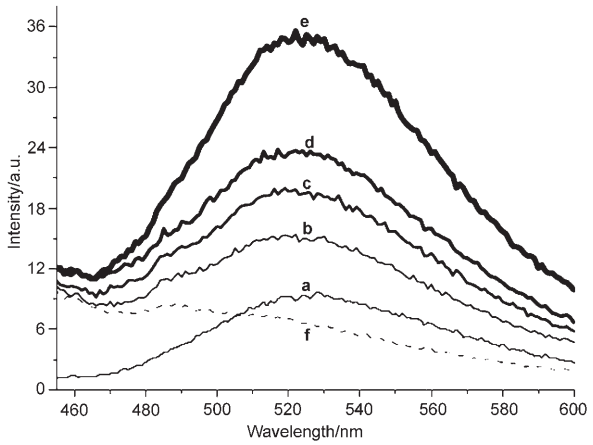

Figure 7. Fluorescent enhancement of **R1**-sol (1.0×10^{-4} M, $\lambda_{ex}=438$ nm) with elevation of gelator content at 40 °C. Gelator content: a) 0%, b) 5%, c) 10%, d) 15%, e) 20%, f) 10% blank.

While it is considered that the photoisomerizations of the dopants will become more difficult if the micelles are very concentrated, we chose our sample-doped hydrosol systems with a 10% gelator content to study their emitting performances accompanied by the photoisomerizations. Variation of fluorescence spectra with respect to the photoisomerization of **R1**-doped hydrosol, **R1**-aq solution, and their references are shown in Figure 8. The fluorescence signals of **R1**-sol and **R1**-ref-sol are both stronger than their corresponding solutions. An increase of emission peak at 395 nm and a decrease of emission peak at 530 nm are both observed in **R1**-sol and **R1**-solution by irradiation at 365 nm for 20 min. Inverse changes of the two peaks takes place by the following irradiation at 254 nm. The fluorescent intensities of the **R1**-ref-sol and **R1**-ref-solution do not change after UV irradiation. These phenomena demonstrate that α-CyD, which has a great influence on the fluorescence of the two stoppers, can shuttle along the linear subunit not only in **R1**-aq solution but also in **R1**-doped hydrosol. Reversible fluorescent alternation of the fluorophores can be induced by the rigidization of the α-CyD ring. Therefore, **R1**-doped hydrosol systems can still perform as a binary switch.

There are two photoisomerizable units in the **R2** molecule, thus three other photostationary states besides the initial state will generate both in alkaline aq solution and hydrosol by irradiation at different wavelengths. The emission spectra of **R2**-doped hydrosol, **R2**-aq solution, and their references are shown in Figure 9. With the photoisomerization

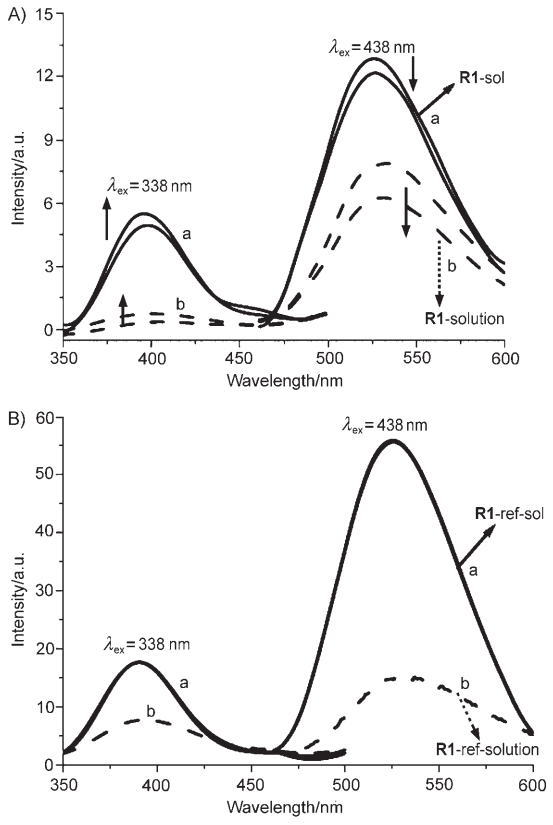

Figure 8. Variation of enhanced fluorescence spectra of **R1**-sol (a; 1.0×10^{-4} M, 40 °C) with continuous irradiation at 365 nm compared with that of **R1**-solution (b, 1.0×10^{-4} M, 25 °C) (A). Enhanced fluorescence spectra of **R1**-ref-sol unvaried (a; 1.0×10^{-4} M, 40 °C) with continuous irradiation at 365 nm compared with that of **R1**-ref-solution (b; 1.0×10^{-4} M, 25 °C) (B).

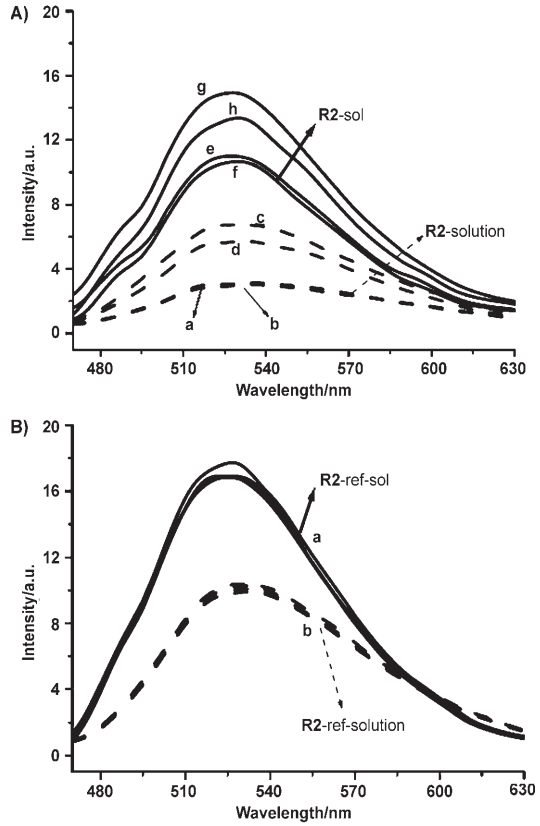

Figure 9. A) Fluorescence emission spectra of four photostationary states of **R2**-sol (alkaline hydrosol 2.1×10^{-5} M, 40 °C) compared with that of **R2**-solution (alkaline aqueous solution 2.1×10^{-5} M, 25 °C). **R2**-solution: a) *EE*, b) *ZE*, c) *EZ*, and d) *ZZ*; **R2**-sol: e) *EE*, f) *ZE*, g) *EZ*, and h) *ZZ*. B) Fluorescence spectra unvaried of **R2**-ref-sol (a; 2.1×10^{-5} M, 40 °C) compared with that of **R2**-ref-solution (b; 2.1×10^{-5} M, 25 °C). a) **R2**-ref-sol, b) **R2**-ref-solution.

of a stilbene unit at 313 nm (*EZ* state), the distance between the ANS unit and α-CyD turns out to be the shortest and an apparently enhanced fluorescence signal is observed. The fluorescent intensity becomes weaker to some extent in other states in the respect that α-CyD is relatively far away from the fluorophore. It is clearly seen that the variations of the fluorescent emission peaks of **R2**-sol and **R2**-solution in Figure 9 meet an identical trend. However, no remarkable fluorescence signal changes of **R2**-ref-sol and **R2**-ref-solution are observed because there is no α-CyD ring located on the dumbbell.

Reversibility and durability of optical fluorescence signals in rotaxane-doped hydrosol–gel systems: Figure 10 shows the changes in ICD signals at 360 nm of **R1**-sol and **R1**-solution

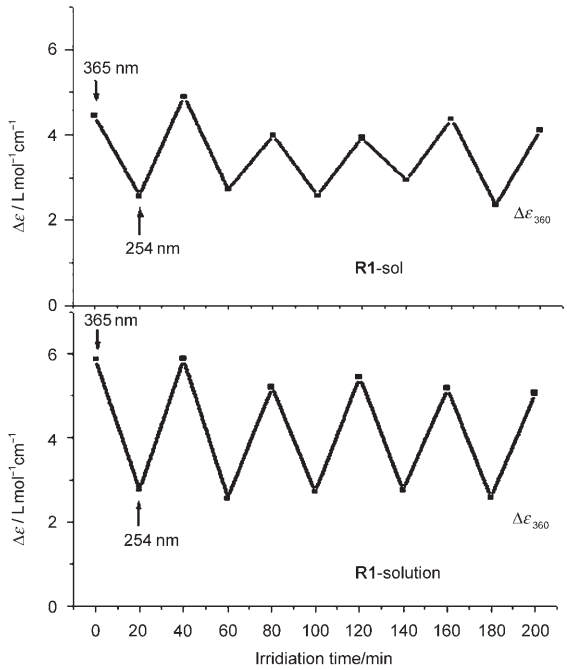

Figure 10. Changes in ICD signals at 360 nm of **R1**-sol with a 10% gelator content (1.0×10^{-4} M, 40 °C) and **R1**-solution (1.0×10^{-4} M, 25 °C) along with changes in irradiation time and light sources. Light sources of 365 and 254 nm UV light were alternated every 20 min.

by irradiation at 365 and 254 nm continuously and alternately. The switching properties of **R1**-doped hydrosol can also reverse well and a good antifatigue ability is displayed as its corresponding solution. This indicates that repeatability of the motion of α-CyD with photoisomerization is not strongly interfered with by the adsorption of micelles. Based on the same conditions of repeatability as the aqueous solution, the rotaxane-doped hydrosol system produces much stronger fluorescent binary signals. In addition to the excellent physical stability of the hydrosol–gel system itself, supermolecular materials will work more effectively in this kind of media.

Conclusion

A type of rotaxane-doped reversible hydrosol–gel system with obvious enhanced fluorescence signals has been prepared. The reversibility of the systems is shown in two aspects. Firstly, the transformation between hydrosol state and hydrogel state controlled by temperature is reversible. Secondly, the variations of optical signals induced by irradiation at different wavelengths in these hydrosol systems are reversible.

ICD spectra have further proved that α-CyD can shuttle along the dumbbell with the photoisomerization of azobenzene or stilbene units. Meanwhile, it has precisely described the change of the angles and positions between the α-CyD ring and the linear subunit. It is sure that keeping nanomaterials like rotaxane in these easily prepared thermoreversible hydrosol–gels will probably build a bridge from molecules to devices for the functional molecules.

Experimental Section

Synthesis: **R1** and **R2** were synthesized by Pd-catalyzed Suzuki coupling in which phenyl boronic acid reacted with phenyl halide in the presence of α-CyD in an Ar-saturated Na_2CO_3 aqueous solution. Chromatography (silica gel, the upper layer was 1.3:2:5 acetic acid/*n*-butanol/water) gave pure target molecules. The non-CyD dumbbell references **R1**-ref and **R2**-ref were also prepared by using the same conditions, in the absence of α-CyD, with the purification by chromatography (silica gel, the upper layer was 1:2:5 acetic acid/*n*-butanol/water). Experimental details of the synthesis and structural characterizations are shown by our former publications (see references [2a, 3d]).

Preparation of rotaxane-doped hydrosol–gel systems: The gelator was a mixture of *N*,*N*,*N*-trimethylhexadecan-1-aminium bromide (**N1**) and an amphoteric surfactant based on quaternary ammonium chloride and sodium sulfonate (**N2**) with a 1:1 molar ratio. An equimolar concentration of **R1**-sol and **R2**-sol was gained by dissolving **R1** and **R2** solid samples in the blank hydrogol (10% mass fraction of dry gelator, namely 10% gelator content) at more than 50 °C. Owing to the temperature-sensitive nature of the amphoteric micelles, **R1**-sol and **R2**-sol can be changed into their corresponding hydrogels by cooling to room temperature and heating back into hydrosols reversibly. The transition temperature of these hydrosol–gel systems is about 30 °C (10% gelator content). Hydrosols can also turn into solutions by heating to a much higher temperature.

Instruments: The ICD spectra were recorded on a Jasco J-815 CD spectrophotometer in a 1 cm quartz cell. H NMR spectra were measured on a Brüker AM 500 spectrometer. UV/visible spectra were carried out by using a Varian Cary 500 spectrophotometer (1 cm quartz cell used). Fluorescent spectra were recorded on a Varian Cary Eclipse Fluorescence spectrophotometer. The photoirradiation was carried by using a CHF-XM 500-W high-pressure mercury lamp with suitable filters in a sealed Ar-saturated 1 cm quartz cell. The distance between the lamp and the sample cell is 20 cm. In hydrogel with 10% gelator content, it takes more or less the same time by continuous irradiations for **R1** and **R2** to reach the photostationary states as their equimolar concentrated aqueous solutions.

Acknowledgement

This work is financially supported by NSFC/China (50673025, 90401026), National Basic Research 973 Program (2006CB806200), partially by the

Education Committee of Shanghai and the Scientific Committee of Shanghai. We thank Professor Bo Fang and his student Qing Yang (Research Laboratory of Chemical Engineering Rheology, ECUST/Shanghai) for their supply of the gelator.

[1] a) V. Balzani, A. Credi, F. M. Raymo, J. F. Stoddart, *Angew. Chem.* **2000**, *112*, 3484–3530; *Angew. Chem. Int. Ed.* **2000**, *39*, 3348–3391; b) V. Balzani, M. Venturi, A. Credi, *Molecular Devices and Machines*, Wiley-VCH, Weinheim (Germany), **2003**; c) G. Wenz, B. H. Han, A. Müller, *Chem. Rev.* **2006**, *106*, 782–817; d) H. Tian, Q. C. Wang, *Chem. Soc. Rev.* **2006**, *35*, 361–374; e) E. R. Kay, D. A. Leigh, F. Zerbetto, *Angew. Chem.* **2007**, *119*, 72–196; *Angew. Chem. Int. Ed.* **2007**, *46*, 72–191.

[2] a) D. H. Qu, Q. C. Wang, J. Ren, H. Tian, *Org. Lett.* **2004**, *6*, 2085–2088; b) E. Katz, O. Lioubashevsky, I. Willner. *J. Am. Chem. Soc.* **2004**, *126*, 15520–15532; c) V. Balzani, M. Clemente-León, A. Credi, B. Ferrer, M. Venturi, A. H. Flood, J. F. Stoddart, *Proc. Natl. Aacd. Sci. USA* **2006**, *103*, 1178–1183; d) W. R. Browne, M. M. Pollard, B. de Lange, A. Meetsma, B. L. Feringa, *J. Am. Chem. Soc.* **2006**, *128*, 12412–12413.

[3] a) C. P. Collier, E. W. Wong, M. Belohradský, F. M. Raymo, J. F. Stoddart, P. J. Kuekes, R. S. Williams, J. R. Heath, *Science* **1999**, *285*, 391–394; b) D. A. Leigh, M. A. F. Morales, E. M. Pérez, J. K. Y. Wong, C. G. Saiz, A. M. Z. Slawin, A. J. Carmichael, D. M. Haddleton, A. M. Brouwer, W. J. Buma, G. W. H. Wurpel, S. León, F. Zerbetto, *Angew. Chem.* **2005**, *117*, 3122–3127; *Angew. Chem. Int. Ed.* **2005**, *44*, 3062–3067; c) D. H. Qu, Q. C. Wang, H. Tian, *Angew. Chem.* **2005**, *117*, 5430–5433; *Angew. Chem. Int. Ed.* **2005**, *44*, 5296–5299; d) D. H. Qu, F. Y. Ji, Q. C. Wang, H. Tian, *Adv. Mater.* **2006**, *18*, 2035–2038.

[4] a) P. N. Taylor, M. J. O'Connell, L. A. McNeill, M. J. Hall, R. T. Aplin, H. L. Anderson, *Angew. Chem.* **2000**, *112*, 3598–3602; *Angew. Chem. Int. Ed.* **2000**, *39*, 3456–3460; b) F. Cacialli, J. S. Wilson, J. J. Michels, C. Daniel, C. Silva, R. H. Friend, N. Severin, P. Samori, J. P. Rabe, M. J. O'Connell, P. N. Taylor, H. L. Anderson, *Nat. Mater.* **2002**, *1*, 160–164; c) J. J. Michels, M. J. O'Connell, P. N. Taylor, J. S. Wilson, F. Cacialli, H. L. Anderson, *Chem. Eur. J.* **2003**, *9*, 6167–6176; d) E. Katz, I. Willner, *Angew. Chem.* **2004**, *116*, 6166–6235; *Angew. Chem. Int. Ed.* **2004**, *43*, 6042–6108.

[5] a) I. Willner, V. Pardo-Yissar, E. Katz, K. T. Ranjit, *J. Electroanal. Chem.* **2001**, *497*, 172–177; b) M. Cavallini, F. Biscarni, S. León, F. Zerbetto, G. Bottari, D. A. Leigh, *Science* **2003**, *299*, 531.

[6] a) E. J. F. Klotz, T. D. W. Claridge, H. L. Anderson, *J. Am. Chem. Soc.* **2006**, *128*, 15374–15375; b) S. Nygaard, K. C. F. Leung, I. Aprahamian, T. Ikeda, S. Saha, B. W. Laursen, S. Y. Kim, S. W. Hansen, P. C. Stein, A. H. Flood, J. F. Stoddart. J. O. Jeppesen, *J. Am. Chem. Soc.* **2007**, *129*, 960–970; c) K. Sakamoto, Y. Takashima, H. Yamaguchi, A. Harada, *J. Org. Chem.* **2007**, *72*, 459–465.

[7] a) Q. C. Wang, D. H. Qu, J. Ren, K. Chen, H. Tian, *Angew. Chem.* **2004**, *116*, 2715–2719; *Angew. Chem. Int. Ed.* **2004**, *43*, 2661–2665; b) D. H. Qu, Q. C. Wang, X. Ma, H. Tian, *Chem. Eur. J.* **2005**, *11*, 5929–5937; c) X. Ma, D. H. Qu, F. Y. Ji, Q. C. Wang, L. L. Zhu, Y. Xu, H. Tian, *Chem. Commun.* **2007**, 1409–1411.

[8] a) R. A. van Delden, M. K. J. ter Wiel, M. M. Pollard, J. Vicario, N. Koumura, B. L. Feringa, *Nature* **2005**, *437*, 1337–1340; b) Y. Liu, A. H. Flood, P. A. Bonvallet, S. A. Vignon, B. H. Northrop, H. R. Tseng, J. O. Jeppesen, T. J. Huang, B. Brough, M. Baller, S. Magonov, S. D. Solares, W. A. Goddard, C. M. Ho, J. F. Stoddart, *J. Am. Chem. Soc.* **2005**, *127*, 9745–9759; c) J. Berná, D. A. Leigh, M. Lubomska, S. M. Mendoza, E. M. Pérez, P. Rudolf, G. Teobaldi, F. Zerbetto, *Nat. Mater.* **2005**, *4*, 704–710; d) Y. Shirai, A. J. Osgood, Y. Zhao, K. F. Kelly, J. M. Tour, *Nano Lett.* **2005**, *5*, 2330–2334.

[9] a) I. C. Lee, C. W. Frank, T. Yamamoto, H. R. Tseng, A. H. Flood, J. F. Stoddart, J. O. Jeppesen, *Langmuir* **2004**, *20*, 5809–5828; b) E. DeIonno, H. R. Tseng, D. D. Harvey, J. F. Stoddart, J. R. Heath, *J. Phys. Chem. B* **2006**, *110*, 7609–7612; c) M. Feng, L. Gao, Z. T. Deng, W. Ji, X. F. Guo, S. X. Du, D. X. Shi, D. Q. Zhang, D. B. Zhu, H. J. Gao, *J. Am. Chem. Soc.* **2007**, *129*, 2204–2205.

[10] a) L. Raehm, J. M. Kern, J. P. Sauvage, C. Hamann, S. Palacin, J. P. Bourgoin, *Chem. Eur. J.* **2002**, *8*, 2153–2162; b) K. Kim, W. S. Jeon, J. K. Kang, J. W. Lee, S. Y. Jon, T. Kim, K. Kim, *Angew. Chem.* **2003**, *115*, 2395–2398; *Angew. Chem. Int. Ed.* **2003**, *42*, 2293–2296; c) H. Azehara, W. Mizutani, Y. Suzuki, T. Ishida, Y. Nagawa, H. Tokumoto, K. Hiratani, *Langmuir* **2003**, *19*, 2115–2123; d) R. Hernandez, H. R. Tseng, J. W. Wong, J. F. Stoddart, J. I. Zink, *J. Am. Chem. Soc.* **2004**, *126*, 3370–3371.

[11] a) K. Murata, M. Aoki, T. Suzuki, T. Harada, H. Kawabata, T. Komori, F. Ohseto, K. Ueda, S. Shinkai, *J. Am. Chem. Soc.* **1994**, *116*, 6664–6676; b) M. de Loos, B. L. Feringa, J. H. van Esch, *Eur. J. Org. Chem.* **2005**, *70*, 3615–3631; c) P. Gao, C. L. Zhan, M. H. Liu, *Langmuir* **2006**, *22*, 775–779; d) X. Ma, Q. C. Wang, D. H. Qu, Y. Xu, F. Y. Ji, H. Tian, *Adv. Funct. Mater.* **2007**, *17*, 829–837; e) N. Fujita, Y. Sakamoto, M. Shirakawa, M. Ojima, A. Fujii, M. Ozaki, S. Shinkai, *J. Am. Chem. Soc.* **2007**, *129*, 4134–4135.

[12] a) L. A. Estroff, A. D. Hamilton, *Chem. Rev.* **2004**, *104*, 1201–1218; b) N. M. Sangeetha, U. Maitra, *Chem. Soc. Rev.* **2005**, *34*, 821–836.

[13] a) G. Bottari, D. A. Leigh, E. M. Pérez, *J. Am. Chem. Soc.* **2003**, *125*, 13360–13361; b) Y. Liu, Y. L. Zhao, H. Y. Zhang, Z. Fan, G. D. Wen, F. Ding, *J. Phys. Chem. B* **2004**, *108*, 8836–8843; c) Y.-B. Han, K. J. Cheng, K. A. Simon, Y. M. Lan, P. Sejwal, Y.-Y. Luk, *J. Am. Chem. Soc.* **2006**, *128*, 13913–13920; d) Q. C. Wang, X. Ma, D. H. Qu, H. Tian, *Chem. Eur. J.* **2006**, *12*, 1088–1096.

[14] a) M. Kodaka, *J. Phys. Chem.* **1991**, *95*, 2110–2112; b) M. Kodaka, *J. Am. Chem. Soc.* **1993**, *115*, 3702–3705; c) M. Kodaka, *J. Phys. Chem. A* **1998**, *102*, 8101–8103.

Received: June 5, 2007
Published online: October 15, 2007

